Diffusion limited aggregation and iterated conformal maps

Benny Davidovitch,[1] H. G. E Hentschel,[2] Zeev Olami,[1] Itamar Procaccia,[1] Leonard M. Sander,[3] and Ellak Somfai[3]
[1]*Department of Chemical Physics, The Weizmann Institute of Science, Rehovot 76100, Israel*
[2]*Department of Physics, Emory University, Atlanta, Georgia 30322*
[3]*H. M. Randall Laboratory of Physics, The University of Michigan, Ann Arbor, Michigan 48109*
(Received 28 July 1998)

The creation of fractal clusters by diffusion limited aggregation (DLA) is studied by using iterated stochastic conformal maps following the method proposed recently by Hastings and Levitov. The object of interest is the function $\Phi^{(n)}$ which conformally maps the exterior of the unit circle to the exterior of an n-particle DLA. The map $\Phi^{(n)}$ is obtained from n stochastic iterations of a function ϕ that maps the unit circle to the unit circle with a bump. The scaling properties usually studied in the literature on DLA appear in a new light using this language. The dimension of the cluster is determined by the linear coefficient in the Laurent expansion of $\Phi^{(n)}$, which asymptotically becomes a deterministic function of n. We find new relationships between the generalized dimensions of the harmonic measure and the scaling behavior of the Laurent coefficients.
[S1063-651X(99)07301-8]

PACS number(s): 64.60.Ak

I. INTRODUCTION

The diffusion limited aggregation (DLA) model was introduced in 1981 by Witten and Sander [1]. The model has been shown to underlie many pattern forming processes including dielectric breakdown [2], two-fluid flow [3], and electrochemical deposition [4]. The model begins with fixing one particle at the center of coordinates in d dimensions, and follows the creation of a cluster by releasing random walkers from infinity, allowing them to walk around until they hit any particle belonging to the cluster. Upon hitting they are attached to the growing cluster. The model was studied on and off lattice in several dimensions $d \geqslant 2$; here we are only interested in the off-lattice versions in two dimensions.

DLA has attracted enormous interest over the years since it is a remarkable example of the spontaneous creation of fractal objects. It is believed that asymptotically (when the number of particles $n \to \infty$) the dimension D of the cluster is very close to 1.71 [5], although there exists to date no accepted proof for this fact in spite of several interesting attempts [6,7]. In addition, the model has attracted interest since it was among the first [8] to offer a true multifractal measure: the harmonic measure (which determines the probability that a random walker from infinity will hit a point at the boundary) exhibits singularities that are usefully described using the multifractal formalism [9]. Nevertheless DLA still poses more unsolved problems than answers. It is obvious that a new language is needed in order to allow fresh attempts to explain the growth patterns, the fractal dimension, and the multifractal properties of the harmonic measure.

Such a new language was proposed recently by Hastings and Levitov [10,11]. These authors showed that DLA in two dimensions can be grown by iterating stochastic conformal maps. We adopt their basic strategy and will see that it provides a new formulation of the problem which may lead to new insights and results.

The basic idea is to follow the evolution of the conformal mapping $\Phi^{(n)}(w)$ which maps the exterior of the unit circle in the mathematical w plane onto the complement of the cluster of n particles in the physical z plane. $\Phi^{(n)}$ is unique by the Riemann mapping theorem, provided that it satisfies the boundary condition

$$\Phi^{(n)}(w) \sim F_1^{(n)} w \quad \text{as} \quad w \to \infty. \tag{1}$$

Here $F_1^{(n)}$ is a real positive coefficient, fixing the argument of $[\Phi^{(n)}(w)]'$ to be zero at infinity. $\Phi^{(n)}(w)$ is related to the complex electric potential $\Psi^{(n)}(z)$ by

$$\Psi^{(n)}(z) = \ln h^{(n)}(z), \tag{2}$$

where $h^{(n)}(z) = [\Phi^{(n)}]^{-1}(z)$ is the inverse mapping. Letting $z \to \infty$ in Eq. (1) it is easy to verify that Eq. (2) implies

$$\Psi^{(n)}(z) \sim \ln z \quad \text{when} \quad z \to \infty \tag{3}$$

as it should be at $d = 2$.

The equation of motion for $\Phi^{(n)}(w)$ is determined recursively. The choice of the initial map $\Phi^{(0)}(w)$ is rather flexible, and in this paper we select (arbitrarily) an initial condition $\Phi^{(0)}(w) = w$. We expect the asymptotic cluster to be independent of this choice. Then suppose that $\Phi^{(n-1)}(w)$ is given. The cluster of n ''particles'' is created by adding a new ''particle'' of constant shape and linear scale $\sqrt{\lambda_0}$ to the cluster of $(n-1)$ ''particles'' at a position which is chosen randomly according to the harmonic measure. We denote points on the boundary of the cluster by $Z(s)$ where s is an arc-length parametrization. The probability to add a particle on an infinitesimal arc ds centered at the point $z(s)$ on the cluster boundary is

$$P(s, ds) \sim |\nabla \Psi(s)| ds. \tag{4}$$

The preimages of $z(s)$ and ds in the w plane are $e^{i\theta}$ and $d\theta$, respectively. Clearly, $ds = |[\Phi^{(n-1)}]'(e^{i\theta})| d\theta$. From Eq. (2) we conclude that

$$P(s, ds) \sim |\nabla \Psi(s)| |\Phi'| d\theta = d\theta, \tag{5}$$

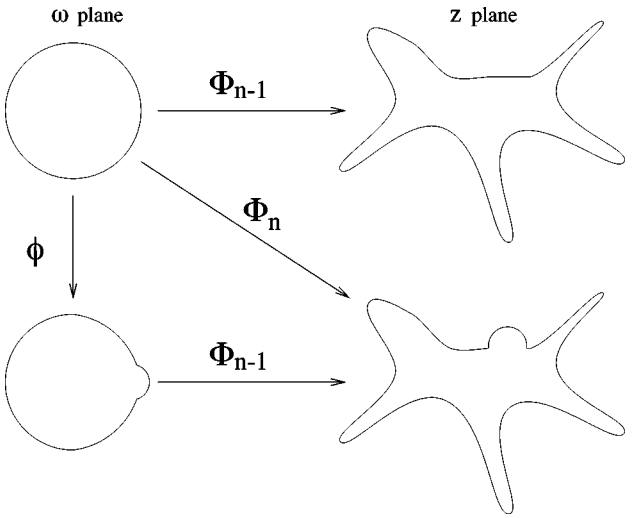

FIG. 1. Diagrammatic representation of the mappings Φ and ϕ.

so the harmonic measure on the real cluster translates to a uniform measure on the unit circle in the mathematical plane.

The image of the cluster of n particles under $h^{(n)}(z)$ is, by definition, just the unit circle. On the other hand, the image of the cluster of n particles under $h^{(n-1)}(z)$ is the unit circle with a small bump whose linear scale is $\sqrt{\lambda_0}/|\Phi'^{(n-1)}(e^{i\theta_n})|$ where $e^{i\theta_n}$ is the image (under $h^{(n-1)}$) of the point z_n on the real cluster at which the growth occurred.

Let us define now a new function $\phi_{\lambda_n,\theta_n}(w)$. This function maps the unit circle to the unit circle with a bump of linear scale $\sqrt{\lambda_n}$ around the point $e^{i\theta_n}$. For $w\to\infty$, $\phi_{\lambda_n,\theta_n}(w)\sim w$ (with positive real proportionality coefficient). Using $\phi_{\lambda_n,\theta_n}(w)$ the recursion relation for $\Phi^{(n)}(w)$ is given by (see Fig. 1)

$$\Phi^{(n)}(w)=\Phi^{(n-1)}(\phi_{\lambda_n,\theta_n}(w)). \tag{6}$$

According to the above discussion λ_n is given by

$$\lambda_n=\frac{\lambda_0}{|\Phi^{(n-1)'}(e^{i\theta_n})|^2} \tag{7}$$

so the right-hand side of Eq. (6) is determined completely by $\Phi^{(n-1)}(w)$; Eq. (6) induces the recursive dynamics of $\Phi^{(n)}(w)$.

The recursive dynamics can be represented as iterations of the map $\phi_{\lambda_n,\theta_n}(w)$,

$$\Phi^{(n)}(w)=\phi_{\lambda_1,\theta_1}\circ\phi_{\lambda_2,\theta_2}\circ\cdots\circ\phi_{\lambda_n,\theta_n}(\omega). \tag{8}$$

This composition appears as a standard iteration of stochastic maps. This is not so. The order of iterations is inverted—the last point of the trajectory is the inner argument in this iteration. As a result the transition from $\Phi^{(n)}(w)$ to $\Phi^{(n+1)}(w)$ is not achieved by one additional iteration, but by composing the n former maps Eq. (8) starting from a different seed which is no longer ω but $\phi_{\lambda_{n+1},\theta_{n+1}}(w)$.

We note that in the physical plane the ''particles'' are roughly of the same size. To achieve this the linear scales $\sqrt{\lambda_n}$ vary widely as a function of n and θ. We will see that the distribution of $\sqrt{\lambda_n}$ and their correlations for different values of n determine many of the scaling properties of the resulting cluster. In particular, their moments are related to the generalized dimensions of the harmonic measure.

There are many functions $\phi_{\lambda,\theta}$ which conformally map the unit circle to the unit circle with a bump. A simple choice is a function which behaves linearly for large w and has a simple pole inside the unit circle which will induce a bump in the image. The pole has to be at $w_0=1-\lambda$ in order to localize the bump near $w=1$ and make it of linear size of the order $\sqrt{\lambda}$. The residue has to be $\lambda^{3/2}$, in order for the bump's height to be also of the order $\sqrt{\lambda}$. Consider then

$$\phi(w)=(1+\lambda)w+\frac{\lambda^{3/2}}{w-w_0}.$$

Careful thinking leads to the conclusion that this function and other similar functions are inappropriate: they have long ''tails.'' In other words, the unit circle is slightly distorted everywhere. This small global distortion may result in a loss of conformality or in the growth of nonconstant size particles in the physical plane in numerical applications.

It was proposed in Ref. [10] that a choice for $\phi_{\lambda_n,\theta_n}(w)$ that is free of global distortion is given by

$$\phi_{\lambda,0}(w)=w^{1-a}\left\{\frac{(1+\lambda)}{2w}(1+w)\times\left[1+w+w\left(1+\frac{1}{w^2}-\frac{2}{w}\frac{1-\lambda}{1+\lambda}\right)^{1/2}\right]-1\right\}^a, \tag{9}$$

$$\phi_{\lambda,\theta}(w)=e^{i\theta}\phi_{\lambda,0}(e^{-i\theta}w). \tag{10}$$

The parameter a is confined in the range $0<a<1$. As a decreases the bump becomes flatter, with the identity map obtained for $a=0$. As a increases towards unity the bump becomes elongated normally to the unit circle, with a limit of becoming a line (''strike'' in the language of [10]) when $a=1$. Naively one might think that the shape of the individual particle is irrelevant for the large scale fractal statistics; we will see that this is not the case. The dependence on a is important and needs to be taken into account. Notice that this map has two branch points on the unit circle. The advantage of this is that the bump is strongly localized. On the other hand, repeated iterations of this map lead to rather complex analytic structure.

The aim of this paper is therefore to investigate the scaling and statistical properties of such iterated stochastic conformal maps with a view to discovering the scaling properties induced by the dynamics which any analytic theory must ultimately explain. In Sec. II we present the numerical procedure used to generate the fractal clusters, and in Sec. III give the necessary mathematical background to describe such mappings. In particular, we discuss the Laurent expansion of the conformal map from the unit circle to the n-particle cluster; the coefficients of the Laurent series have

FIG. 2. Typical clusters of 10 000 particles. The black regions represent the interiors of the images of the unit circle under the map $\Phi^{(10\,000)}$ for three values of a. The large enclosed areas for the $a=\frac{1}{2}$ cluster are the unwanted ''fillup'' events discussed in Sec. II. However, the black area in the $a=\frac{4}{5}$ cluster is only a numerical artifact: that region is not resolved by double precision arithmetic.

interesting scaling behavior with the size of the cluster which is intimately related to the fractal dimension of the cluster and to the generalized dimensions of the harmonic measure. In Sec. IV we present numerical results regarding the scaling properties of averages of the Laurent coefficients and of the size parameter λ_n. The results are accompanied by a theoretical analysis and interpretation. In Sec. V we conclude with some remarks on the road ahead.

II. NUMERICAL PROCEDURE

The algorithm simulating the growth of the cluster is based on Ref. [10]. The n-''particle'' cluster is encoded by the series of pairs $\{(\theta_i,\lambda_i)\}_{i=1}^{n}$. Having the first $n-1$ pairs, the nth pair is found as follows: choose θ_n from a uniform distribution in $[0,2\pi]$, independent of previous history. Then compute λ_n from Eq. (7), where the derivative of the iterated function $\Phi^{(n-1)}$ involves $\phi'_{\lambda_{n-1},\theta_{n-1}}$, $\phi'_{\lambda_{n-2},\theta_{n-2}}$, $\phi'_{\lambda_{n-3},\theta_{n-3}}$ etc., computed, respectively, at the points $e^{i\theta_n}$, $\phi_{\lambda_{n-1},\theta_{n-1}}(e^{i\theta_n})$, $\phi_{\lambda_{n-2},\theta_{n-2}}(\phi_{\lambda_{n-1},\theta_{n-1}}(e^{i\theta_n}))$, etc. Notice that the evaluation of both Φ' and Φ after the addition of one particle involves $O(n)$ operations since the seed changes at every n. This translates into n^2 time complexity for the growth of an n-particle cluster. This is inferior to the best algorithms to grow DLA (using hierarchical maps [12], with close to linear efficiency), but the present algorithm is not aimed at efficiency. Rather, it is used since the Laplacian field and the growth probability which is derived from it are readily available at every point of the cluster and away from it. The typical time to grow a 10 000-particle cluster is 8 minutes on a 300 MHz Pentium-II.

Naively one would expect that any choice of $0<a<1$ would yield DLA clusters, since a only determines the shape of the particles [the aspect ratio is $\frac{1}{2}a/(1-a)$ for small λ], and the microscopic details of the particles (except their linear size) should not affect the global properties. Three typical clusters with particles of various aspect ratios a are shown in Fig. 2. We mark in black the interior of the image of the unit circle under the conformal map $\Phi^{(n)}(w)$. The objects look very much like typical DLA clusters grown by standard off-lattice techniques, and in the next section we demonstrate that they have fractal dimensions in close agreement with the latter. For a significantly different from 2/3, disadvantages of the algorithm get amplified. Since the functional form of ϕ is fixed (only the size and position of the ''bump'' change), particles of constant shape and size are obtained only if the magnification factor $|\Phi^{(n-1)'}|$ (the inverse of the field) is approximately constant in the w plane around the ''bump'' of ϕ. If the particles are elongated along the cluster, then the variation of the field along the cluster affects the shape: large otherwise deeply invaginated regions, where Φ' is large, are filled up with a single particle, and the resulting cluster tends to be more compact. This effect, slightly noticeable even at $a=2/3$, is quite significant at the otherwise natural choice of $a=1/2$, where the particles are half circles. In Fig. 2 we show such a cluster and point out the area filling dark regions which represent such unwanted events. The other extreme, when the particles stick out of the cluster, leads to sensitivity to variations in the field going *away* from the cluster. Especially if a bump is grown on a tip of a branch, where the field decreases rapidly as one goes away from the tip (such that Φ' increases significantly), then the map of the bump gets magnified, resulting in particles of very unequal sizes.

It is necessary to stress that even for $a=2/3$, when this procedure appears to yield nice ramified structures, the problem of fill-ups does not go away: in a few rare cases the particle—if it happens to land on a place where $|\Phi''|$ is large—is significantly distorted. The net effect is that large areas surrounded by the cluster (where the growth probability is small) are filled up entirely by one distorted particle. For the value of $a=1/2$ it appeared that the errors may be unbounded. Our numerics indicates that for $a=2/3$ the errors were bounded for the cluster sizes that we considered. We do not have a mathematical proof of boundedness of the errors, and our disregard of this danger is only based on the sensible appearance of our clusters at this value of a.

III. MATHEMATICAL BACKGROUND

In this section we discuss the Laurent expansion of our conformal maps, and introduce the statistical objects that are studied numerically in the next section.

A. Laurent expansion

Since the functions $\Phi^{(n)}(w)$ and $\phi_{\lambda,\theta}(w)$ are required to be linear in w at infinity, they can be expanded in a Laurent series in which the highest power is w:

$$\Phi^{(n)}(w)=F_1^{(n)}w+F_0^{(n)}+F_{-1}^{(n)}w^{-1}+F_{-2}^{(n)}w^{-2}+\cdots, \tag{11}$$

$$\phi_{\lambda,\theta}(w)=f_1w+f_0+f_{-1}w^{-1}+f_{-2}w^{-2}+\cdots, \tag{12}$$

where

$$f_1=(1+\lambda)^a,$$

$$f_0=\frac{2a\lambda e^{i\theta}}{(1+\lambda)^{1-a}},$$

$$f_{-1}=\frac{2a\lambda e^{2i\theta}}{(1+\lambda)^{2-a}}\left(1+\frac{2a-1}{2}\lambda\right),$$

$$f_{-2}=\frac{2a\lambda e^{3i\theta}}{(1+\lambda)^{3-a}}\left(1+2(a-1)\lambda+\frac{2a^2-3a+1}{3}\lambda^2\right).$$

The recursion equations for the Laurent coefficients of $\Phi^{(n)}(w)$ can be obtained by substituting the series of Φ and ϕ into the recursion formula (6). We find

$$F_1^{(n)}=F_1^{(n-1)}f_1^{(n)}, \tag{13}$$

$$F_0^{(n)}=F_1^{(n-1)}f_0^{(n)}+F_0^{(n-1)},$$

$$F_{-1}^{(n)}=F_1^{(n-1)}f_{-1}^{(n)}+F_{-1}^{(n-1)}/f_1^{(n)}, \tag{14}$$

$$F_{-2}^{(n)}=F_1^{(n-1)}f_{-2}^{(n)}-F_{-1}^{(n-1)}\frac{f_0^{(n)}}{(f_1^{(n)})^2}+F_{-2}^{(n-1)}\frac{1}{(f_1^{(n)})^2}.$$

We note that the n dependence of $f_i^{(n)}$ follows from the dependence on the randomly chosen θ_n at the nth step, from which follows the dependence of λ_n on n. The latter is, however, a function of all the previous growth steps, making the iteration (13),(14) rather difficult to analyze.

A general relation between the Laurent coefficients is furnished by the so-called area theorem which applies to univalent mappings. Since our maps solve the Laplace equations with boundary conditions only at infinity and on the cluster boundary where the potential is zero, they map the w plane uniquely (and with a unique inverse) to the z plane. In other words, the pressure lines and the stream lines are nondegenerate. Such mappings have the property [13] that the area of the image of the unit disk in the nth step is given by

$$S_n=|F_1^{(n)}|^2-\sum_{k=1}^{\infty}k|F_{-k}^{(n)}|^2. \tag{15}$$

A second theorem that will be useful in our thinking is a consequence of the so-called one-fourth theorem, see Appendix A. There a statement is proven that the interior of the curve $\{z:z=\Phi^{(n)}(e^{i\theta})\}$ is contained in the z plane by a circle of radius $4F_1^{(n)}$. Now as the area S_n is obtained simply from the superposition of n bumps of roughly the same area λ_0, it has to scale as $S_n\approx n\lambda_0$, for large n. On the other hand, any typical radius of the cluster should scale as $n^{1/D}\sqrt{\lambda_0}$ where D is the dimension of the cluster. We can thus expect a scaling of $F_1^{(n)}$ that goes as

$$F_1^{(n)}\sim n^{1/D}\sqrt{\lambda_0}. \tag{16}$$

We note in passing that this scaling law offers us a very convenient way to measure the fractal dimension of the growing cluster. Indeed, we measured the dimension D for a range of a in this way by averaging $F_1^{(n)}$ over 100 clusters. We found that for a range of a spanning the interval [1/3,8/9] the dimension is constant, around 1.7.

We can infer from Eq. (16) that the sum in Eq. (15) which subtracts positive contributions from $|F_1^{(n)}|^2$ contains terms that cancel the behavior of $n^{2/D}$ (remember that $D<2$), leaving a power of unity for the scaling of S_n. Indeed, we will show below both numerical and theoretical evidence for the scaling behavior of the $|F_{-k}^{(n)}|^2$ for $k>6$ which is in agreement with $n^{2/D}$.

We can give a direct physical interpretation for the coefficients $F_k^{(n)}$ by comparing them to the coefficients of the series for $\Psi^{(n)}$, cf. Eq. (2):

$$\Psi^{(n)}(z)=\ln(z)-\ln(r_0)+\sum_1^{\infty}\frac{\psi_k}{z^k}. \tag{17}$$

The coefficient of $\ln(z)$ is unity so that the electric flux is unity. This corresponds to the normalization of the probability. The constant r_0 is the Laplace radius which is the radius of a charged disk which would give the same field far away. The rest of the ψ_k's are conventional multipole moments.

The relations between the Laurent coefficients of $\Psi^{(n)}$ and $\Phi^{(n)}$ are

$$r_0=F_1,$$

$$\psi_1=-F_0,$$

$$\psi_2=-F_{-1}F_1-\frac{1}{2}F_0^2, \tag{18}$$

$$\psi_3=-F_{-2}F_1^2-2F_0F_{-1}F_1-\frac{1}{3}F_0^3,$$

$$\psi_4=-F_{-3}F_1^3-\frac{3}{2}F_{-1}^2F_1^2-3F_1F_0^2F_{-1}-3F_{-2}F_0F_1^2-\frac{1}{4}F_0^4.$$

The first line shows that $F_1=r_0$, the Laplace radius, in accordance with the one-fourth theorem.

The second line shows that the dipole moment ψ_1 is $-F_0$. We can interpret this coefficient as a distance, the wandering of the center of charge due to the random addition of the particles. We will take the point of view that this quantity is less ''intrinsic'' than the others to the dynamics of the DLA growth. In fact, if we set $F_0=\psi_1=0$ (we could imagine shifting the cluster as we grow it), we can rewrite the rest of the equations:

$$-F_{-1}\sim\psi_2/r_0,$$

$$-F_{-2}\sim\psi_3/r_0^2, \tag{19}$$

$$-F_{-3}\sim(\psi_4+\tfrac{3}{2}\psi_2^2)/r_0^3,$$

etc. This leads to the interpretation of F_{-k} in terms of the multipole expansion of the electric field.

B. Statistical objects and the relations to generalized dimensions

Our growth process is stochastic. Accordingly, it is natural to introduce averages over the randomness. In our thinking there are two important averages, one over histories of the whole random trajectory $\{\theta_i\}_{i=1}^{n}$, and the other only over the random choice of θ_n at the nth step. To distinguish between the two we denote the first by angular brackets and refer to it as ''history average,'' while the second is denoted by an overbar and referred to as a ''cluster average.'' There is a possibility that for very large clusters ($n\to\infty$) the two averages result in the same numbers. We will refer to such a property as ''self-averaging.''

The cluster average of moments of λ_n offers a relationship to the generalized dimensions of the harmonic measure [14]. The latter are defined by dividing the plane into boxes of size ϵ, and estimating the probability for a random walker to hit the piece of the boundary of the cluster which is included in the ith box by

$$p_i(\epsilon)=|E_i|\epsilon, \tag{20}$$

where $|E_i|$ is the modulus of the electric field $|\nabla\Psi_i|$ at some point in the ith box. The generalized dimensions are defined by the relation

$$\sum_{i=1}^{N(\epsilon)} p_i^q(\epsilon)\sim\left(\frac{\epsilon}{R}\right)^{(q-1)D_q}, \tag{21}$$

where $N(\epsilon)$ is the number of boxes of size ϵ that are needed to cover the boundary, and R is the linear size of the largest possible box, which is of the order of the radius of the cluster. Substituting Eq. (20) we find

$$\epsilon^{q-1}\sum_{i=1}^{N(\epsilon)} |E_i|^q\epsilon\sim\left(\frac{\epsilon}{R}\right)^{(q-1)D_q}. \tag{22}$$

Taking ϵ very small, of the order of $\sqrt{\lambda_0}$, and assuming that the field is smooth on this scale we have

$$\int_0^L |E_i|^q ds\sim(\sqrt{\lambda_0})^{1-q}\quad n^{(1-q)D_q/D}, \tag{23}$$

where L is the length of the boundary, ds is an arc-length differential, and we have used the scaling law $n\sim S_n/\epsilon^2\sim(R/\epsilon)^{1/D}$.

The connection to our language is obtained by considering the cluster average of powers of λ_n. We grow a cluster of $n-1$ particles, perform repeated random choices of growth sites (without growing), and compute λ_n for each choice. The cluster average can be represented as an integral over the unit circle, $\overline{\lambda_n^q}$, and is given by

$$\overline{\lambda_n^q}\equiv(1/2\pi)\int_0^{2\pi}\lambda_n^q(\theta)d\theta. \tag{24}$$

Recalling Eq. (7) we observe that $\lambda_n^q(\theta)=\lambda_0^q|E(\theta)|^{2q}$. The last relation, Eq. (5), and Eq. (23) imply the scaling relation

$$\overline{\lambda_n^q}\sim n^{-2qD_{2q+1}/D}. \tag{25}$$

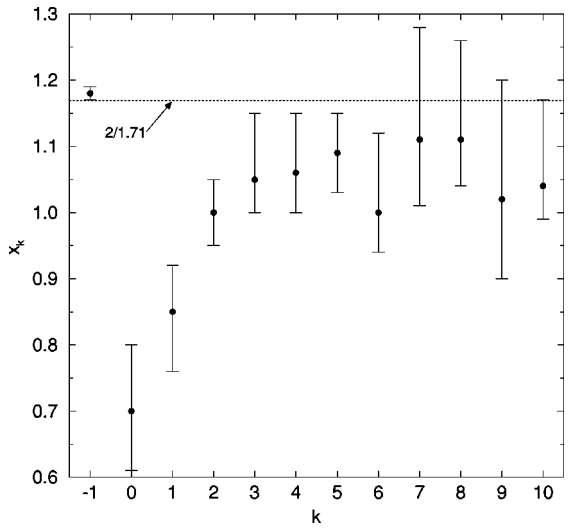

FIG. 3. The scaling exponents of the Laurent coefficients: $\langle|F_{-k}|^2\rangle\sim n^{x_k}$. The values are obtained by averaging 400 independent realizations of 10 000 particle clusters.

IV. NUMERICAL RESULTS AND THEIR INTERPRETATION

In this section we present results on three topics.

(i) The coefficients of the Laurent expansion. The scaling behavior of these quantities is described and discussed in Sec. IV A.

(ii) The microscopic fluctuations in the conformal map. We show that the assumption of self-averaging is valid for Eq. (25) and that the multifractal exponents are in a good agreement with the known ones.

(iii) Distribution functions of the Laurent coefficients. We analyze numerically the width of those functions and find that $F_1^{(n)}$ tends to a deterministic function of n. We attribute this effect to nontrivial temporal correlations in the field, and give some evidence of their existence.

A. Laurent coefficients of $\Phi^{(n)}$

All the coefficients of the Laurent series of $\Phi^{(n)}(w)$ are complex numbers except F_1 which is real by the choice of zero phase at infinity, see Eq. (1). Most of our discussion below pertains to the amplitudes of the coefficients F_k. We need to stress, however, that the phases are not irrelevant. If we attempted to use the correct amplitudes with random phases, the resulting series will in general not be conformal.

One of the main results of this paper is that in addition to the expected scaling behavior of the linear coefficient $F_1^{(n)}$ [given in Eq. (16)] the rest of the amplitudes of the Laurent coefficients $|F_{-k}^{(n)}|$ exhibit also a scaling behavior. We find numerically that in the mean the magnitudes of the Laurent coefficients scale as powers of n:

$$\langle|F_k^{(n)}|^2\rangle=a_k n^{x_k}. \tag{26}$$

The exponents x_k are given in Fig. 3. We first discuss the consequences of the scaling behavior of $F_1^{(n)}$.

1. Scaling of F_1

The scaling behavior (16) has immediate consequences for the scaling behavior of the bump areas λ_n. The connec-

tion appears from the recursion Eq. (13) of $F_1^{(n)}$ which together with $f_1=(1+\lambda)^a$ reads

$$F_1^{(n)}=\prod_{k=1}^{n}[1+\lambda_k]^a. \tag{27}$$

Taking history averages we find

$$\langle F_1^{(n)}\rangle=\left\langle \prod_{k=1}^{n}[1+\lambda_k]^a \right\rangle, \tag{28}$$

$$\ln\langle F_1^{(n)}\rangle \approx a\sum_{k=1}^{n}\langle\lambda_k\rangle, \tag{29}$$

$$d\ln\langle F_1^{(n)}\rangle/dn \approx a\langle\lambda_n\rangle. \tag{30}$$

The last two equations are obtained by expanding the logarithm and keeping only divergent sums: both the mean of $F_1^{(n)}$ and the mean of the sum of λ_k increase as a function of n. All other sums of powers of λ_k converge as a function of n, cf. Sec. IV B. Thus, if we assume that $\langle F_1^{(n)}\rangle \propto n^{1/D}$, cf. Eq. (16), fractal scaling of the radius (see below) implies that [10]

$$\langle\lambda_n\rangle = 1/naD. \tag{31}$$

In the next subsection we show that this is indeed supported by the simulations. Note that $\langle\lambda_n\rangle$ is inversely proportional to n for any value of the fractal dimension D. On the other hand, if we assume the property of self-averaging, Eq. (31) implies a relationship between the generalized dimension D_3 and the fractal dimension D. Comparing Eqs. (25) and (31) leads immediately to the relation

$$D_3 = D/2. \tag{32}$$

This scaling relation was derived by Halsey [15] using much more elaborate considerations. We see that in the present formalism this scaling relation is obtained very naturally. In fact the present formulation is more powerful since Eq. (31) predicts not only the exponent of the third moment of the electric field, but also the prefactor. It is also noteworthy that the scaling relation (32) results simply from the existence of a power law behavior for the radius $F_1^{(n)}$.

2. Scaling of F_0

We found the exponent of $\langle|F_0|^2\rangle$ to be $x_0=0.7\pm0.1$, see Fig. 4. To estimate the scaling behavior of F_0 theoretically we note that

$$F_0=\frac{1}{2\pi}\int_0^{2\pi}\Phi^{(n)}(\theta)d\theta=\frac{1}{2\pi}\int_0^L z(s)|E(s)|ds. \tag{33}$$

Accordingly we can write

$$\overline{|F_0|^2}=(1/4\pi^2)\int_0^L ds\int_0^L ds'\,\overline{z(s)z(s')^*|E(s)||E(s')|}$$

$$\sim\lambda_0 R^2\int_0^L ds|E(s)|^2. \tag{34}$$

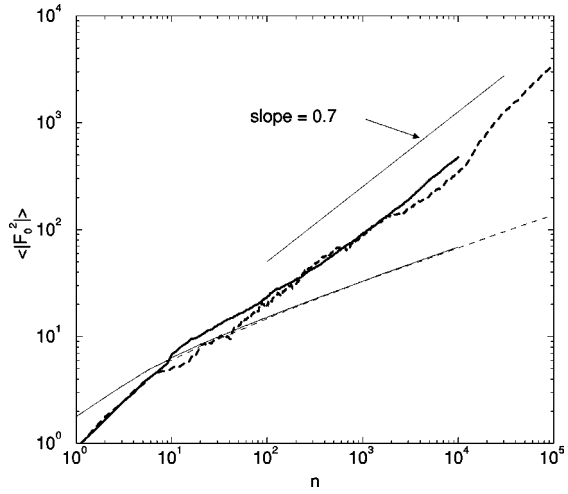

FIG. 4. The scaling of $\langle|F_0^{(n)}|^2\rangle$ (thick lines) and the sum of diagonal terms [thin lines, see Eq. (51)] with size n. Clearly the two have different scaling exponents. The solid lines are averages over 400 clusters of size 10 000, the dashed lines are averages over 30 clusters of size 100 000.

In writing the second line we assumed that the main contribution to the correlation function is short ranged,

$$\langle z(s)z(s')^*|E(s)||E(s')|\rangle\sim\lambda_0 R^2\overline{|E(s)|^2}\delta(s-s'). \tag{35}$$

The justification for this is that the field is expected to exhibit wild variations as we trace the boundary $z(s)$. In addition the main contribution to the integral is expected to come from the support of the harmonic measure where the radius is of the order of R. From the estimate (34) and Eq. (23) we then find

$$x_0=\frac{2-D_2}{D}\approx 0.64 \tag{36}$$

in agreement with our measurement of x_0. (We used here $D_2=0.90$ in correspondence with the numerical finding reported in Sec. IV C. Any of the values of D_2 quoted in the literature would yield x_0 in the range 0.7 ± 0.1.)

3. Scaling of F_{-k}

The exponents x_k for $k<0$ are smaller than $2/D$ but approach it asymptotically, see Fig. 3. This behavior is expected from the area theorem, and also from a direct estimate of the integral representation of the coefficients for large k,

$$\overline{|F_{-k}|^2}=\frac{1}{4\pi^2}\int_0^L ds \times\int_0^L ds'\,\overline{z(s)z(s')^*|E(s)||E(s')|e^{ik[\theta(s)-\theta(s')]}}. \tag{37}$$

In Appendix B we show that this integral can be estimated using the multifractal formalism of the harmonic measure with the final result

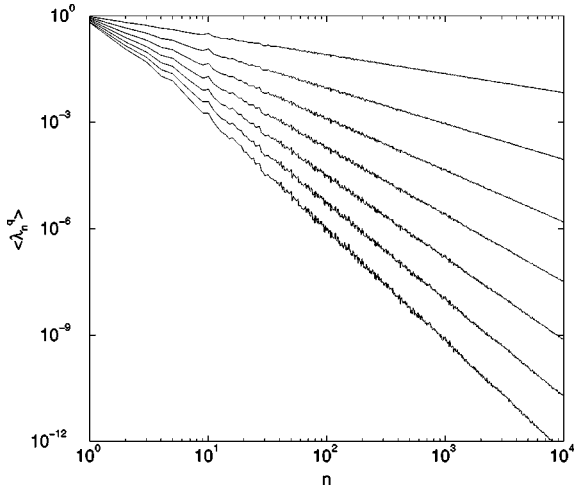

FIG. 5. Scaling of the moments $\langle \lambda_n^q \rangle$ with powers of n. The curves from top to bottom correspond to $q=0.5, 1, 1.5, 2, 2.5, 3,$ and 3.5. The exponents $-2qD_{2q+1}/D$ are in agreement with theoretical predictions (see text) and with numerical values for the generalized dimensions in the literature.

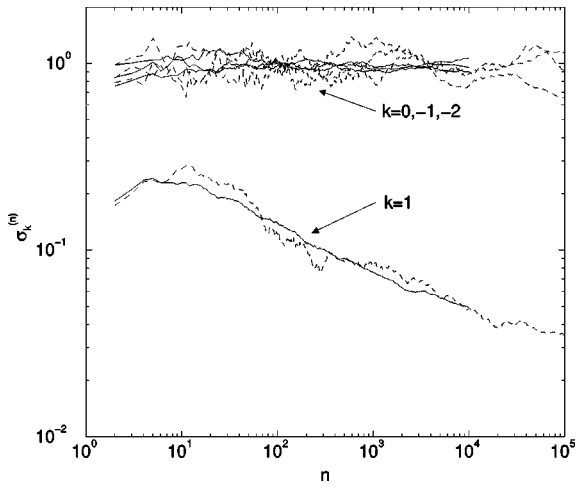

FIG. 6. The rescaled standard deviation $\sigma_k^{(n)}$ of the Laurent coefficients of the map (see definition in text). For $k \neq 1$, $\sigma_k^{(n)}$ fluctuates around unity, corresponding to broad distributions. For $k=1$ it tends to zero as $n \to \infty$, demonstrating the asymptotic sharpness of the distribution of F_1. The solid lines are averages over 400 clusters of size 10 000, the dashed lines are averages over 30 clusters of size 100 000.

$$\overline{|F_{-k}|^2} \sim (R/4k)^2 \int d\alpha (2k/\pi)^{f(\alpha)/\alpha}, \tag{38}$$

where α and $f(\alpha)$ are the strength of singularities of the harmonic measure and the dimension of the sets of points that exhibit these singularities, respectively [9]. For our purposes the important consequence of Eq. (38) is the scaling relation (assuming self-averaging)

$$\langle |F_{-k}|^2 \rangle = \lambda_0 n^{2/D} g(k), \tag{39}$$

with $g(k) \sim 1/k^2 \int d\alpha\, k^{f(\alpha)/\alpha}$. One knows from the theory of multifractals that $f(\alpha)/\alpha \leqslant 1$, and therefore we can bound $g(k)$ from above and from below, $Ak^{-2} < g(k) < Bk^{-1}$. This is in accord with our numerical simulations in the range $3 \leqslant k \leqslant 10$, although the calculation in Appendix B is only valid for large values of k. We found agreement with Eq. (26) with $x_k \to 2/D$ and $a_k \sim k^{-\alpha}$ with $1 < \alpha < 2$.

Note that this scaling behavior has important consequences for both the area theorem and for conformality. Absolute convergence of the sum $\Sigma_{k=1}^{\infty} k|F_{-k}^{(n)}|^2$ in the area theorem requires $\alpha > 2$, which is not the case. The situation is even more serious for the existence of conformality. To ensure the latter the sum $\Sigma_{k=1}^{\infty} k|F_{-k}^{(n)}|$ must exist. This would require $\alpha > 4$. The reason that the sums exist in the theory is only due to the ultraviolet cutoff at $\sqrt{\lambda_0}$. This cutoff introduces a highest k in the Laurent expansion which we estimate as $2\pi k_{\max} \approx L/\sqrt{\lambda_0} \sim n$ where L is the perimeter of the cluster.

B. Multifractal exponents

Here we test Eq. (25). In Fig. 5 we display double-logarithmic plots of $\langle \lambda_n^q \rangle$ vs n for $q=0.5$, 1, 1.5, 2, 2.5, 3, and 3.5. The values of the exponents derived from our simulations agree very well (within the uncertainties) with the generalized dimensions D_q obtained in the past [5] for $D_2, \ldots, D_8$ using standard methods. In addition we reproduce numbers in agreement with the theoretical prediction of $D_0 = D \approx 1.71$ and $D_3 = D/2$. This agreement is a strong indication for self-averaging at least for the purpose of computing moments of λ_n (i.e., $\langle \lambda_n^q \rangle \sim \overline{\lambda_n^q}$).

C. Fluctuations of the averages

We previously discussed the scaling behavior of $|F_{-k}^{(n)}|^2$ and showed that their history averages obey Eq. (26). However, $|F_{-k}^{(n)}|$ are random variables with broad scaling distributions. Figure 6 describes the rescaled standard deviation $\sigma_k^{(n)}$ of the Laurent coefficients,

$$\sigma_k^{(n)} = \sqrt{\langle |F_k^{(n)}|^4 \rangle - \langle |F_k^{(n)}|^2 \rangle^2} / \langle |F_k^{(n)}|^2 \rangle, \tag{40}$$

for $k = 1, 0, -1, -2$ as a function of the cluster size n. As is seen clearly from the graphs the widths of the distributions for all $k \leqslant 0$ tend asymptotically to a finite value. This is the normal behavior for scaling distributions. The exceptional case is $k=1$. Even though it exhibits a scaling law of the type (26) (see Sec. III), with

$$x_1 = \frac{2}{D} \approx 1.18,$$

the rescaled distribution width of $|F_1^{(n)}|^2$ tends to zero as n goes to infinity. This means that the rescaled distribution function of $F_1^{(n)}$ tends asymptotically to a δ function. The importance of this result for the evaluation of the fractal dimension of the cluster warrants an immediate discussion of this sharpening phenomenon.

The conclusion of the numerics on F_1 is that there exists a universal constant $c(\lambda_0)$ such that

$$n^{-1/D} F_1^{(n)} \to c(\lambda_0), \tag{41}$$

where $c(\lambda_0)$ is cluster independent. Moreover, we found that $c(\lambda_0) = c\sqrt{\lambda_0}$, which is in accordance with the role played

by $\sqrt{\lambda_0}$ as an ultraviolet inner length scale, which is the only length scale that appears in the mappings. Note that the constant c in Eq. (41) depends on the parameter a. We measured c values of 0.6, 0.87, 1.2, and 1.8 for a values of 1/3, 1/2, 2/3, and 4/5, respectively.

The observed sharpening is not obvious since we know that $F_1^{(n)}$ is built from a product of random variables λ_n, whose moments change with n in multifractal manner according to Eq. (25).

One could attempt to connect the sharpening of $F_1^{(n)}$ to the existence of other sharp functions of n. Considering the full expansion of Eq. (27) we find

$$\frac{1}{a}\ln F_1^{(n)} = \sum_{i=1}^{n} \ln(1+\lambda_i) = \sum_{i=1}^{n} \lambda_i - \frac{1}{2}\sum_{i=1}^{n} \lambda_i^2 + \frac{1}{3}\sum_{i=1}^{n} \lambda_i^3 + \cdots . \tag{42}$$

We could understand Eq. (41) easily if all the sums of all the powers of λ_i converged to constants,

$$\sum_{i=1}^{n} \lambda_i - \frac{2}{D}\ln n \to c_1 , \tag{43}$$

$$\sum_{i=1}^{n} \lambda_i^2 \to c_2 , \tag{44}$$

with c_i cluster independent. In fact, this is not the case. The sums of powers are not cluster independent. A clear demonstration of this is a simulation that we performed in which the initial condition was very far from a circle. The individual sums in Eq. (42) were very different from the average values, but nevertheless $\Sigma_{i=1}^{n}\ln(1+\lambda_i)$ converged to the right value. It is our conclusion that each of the sums in Eq. (42) is not cluster independent, and yet somehow the resummed form is cluster independent.

This remarkable sharpening calls for further discussion; it appears that its interpretation requires better understanding of the time correlations of the field: an independent choice of random realization of a series of λ_i according to their multifractal distribution can only generate $F_1^{(n)}$ with the proper scaling exponent but cannot trivially yield a highly peaked distribution of $F_1^{(n)}$. Therefore we consider now some evidence for the existence of temporal correlations.

The first outstanding evidence appears in the context of the scaling behavior of F_0, which was discussed in Sec. IV A. We show that if we assume that there exist no correlations between different growth stages, the exponent x_0 will be very different from the measured and calculated value. From the recursion relations of the Laurent coefficients [Eq. (14)] we can estimate, in the limit of large n when λ_n is very small on the average,

$$\langle |F_0^{(n)}|^2 \rangle \sim \sum_{m=1}^{n}\sum_{m'=1}^{n} \langle F_1^{(m)} F_1^{(m')} \lambda_m \lambda_{m'} e^{i(\theta_m - \theta_{m'})} \rangle \sim \sum_{m=1}^{n}\sum_{m'=1}^{n} \langle F_1^{(m)} F_1^{(m')} \rangle \langle \lambda_m \lambda_{m'} e^{i(\theta_m - \theta_{m'})} \rangle . \tag{45}$$

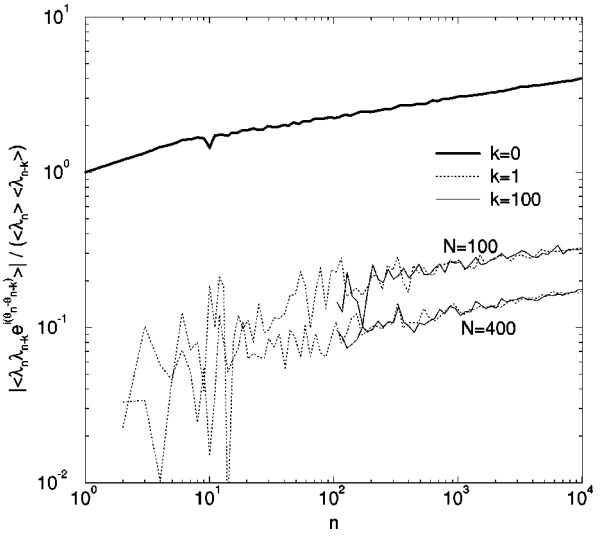

FIG. 7. Time-angle correlations of the field. In order to reduce statistical noise, the values plotted are averaged in bins $[n, 1.1n]$.

The second line is obtained because $F_1^{(m)}$ is proportional to the radius of the whole cluster and should not be correlated with λ_m. The crucial approximation comes next: if λ_m and $\lambda_{m'}$ can be treated as independent for $m \neq m'$, then (since θ_m and $\theta_{m'}$ are independent) Eq. (45) simplifies to

$$\langle \lambda_m \lambda_{m'} e^{i(\theta_m - \theta_{m'})} \rangle \approx \langle \lambda_m^2 \rangle \delta_{m,m'} \tag{46}$$

$$\langle |F_0^{(n)}|^2 \rangle \sim \sum_{m=1}^{n} \langle (F_1^{(m)})^2 \rangle \langle \lambda_m^2 \rangle \sim n^{1+2/D-4D_5/D} \sim n^{0.3} . \tag{47}$$

The numerical simulation resulted in an exponent of the order of 0.7, in serious disagreement with Eq. (47). We think that the assumption of independence, Eq. (46), is the culprit.

Another fact which illustrates the importance of the time-angle correlation Eq. (46) is the difference between the exponents of F_0 and F_{-1} ($\langle |F_0|^2 \rangle \sim n^{0.7}$ whereas $\langle |F_{-1}|^2 \rangle \sim n^{0.9}$). Their equations of motion (14) differ, for small λ_n, by two terms only. The first one is the term $\lambda_n F_{-1}^{(n-1)}$ in the right hand side of the equation for F_{-1} which is absent in the equation for F_0. We checked numerically that neglecting this term leads to a very small change in the exponent. The second difference is that the term $\lambda_n \lambda_{n-k} e^{i(\theta_n - \theta_{n-k})}$ in Eq. (48) is replaced by $\lambda_n \lambda_{n-k} e^{2i(\theta_n - \theta_{n-k})}$. The change in the exponent can therefore be directly attributed to the existence of important time-angle correlations.

We tried to analyze numerically the time-angle correlations $\langle \lambda_n \lambda_{n-k} e^{i(\theta_n - \theta_{n-k})} \rangle$. The results for some k's are shown in Fig. 7. It appears that as we increase the size of the ensemble, $\langle \lambda_n \lambda_{n-k} e^{i(\theta_n - \theta_{n-k})} \rangle \to 0$ with the usual $N^{-1/2}$ dependence on the ensemble size. If we believe these numerical results (doubts may exist due to the relative smallness of the ensembles analyzed), then the previous results must be related to more subtle correlation of higher order nature.

Lastly we would like to discuss the importance of early stages of the growth. $\langle F_1^{(n)} \rangle$ might be written in the following way:

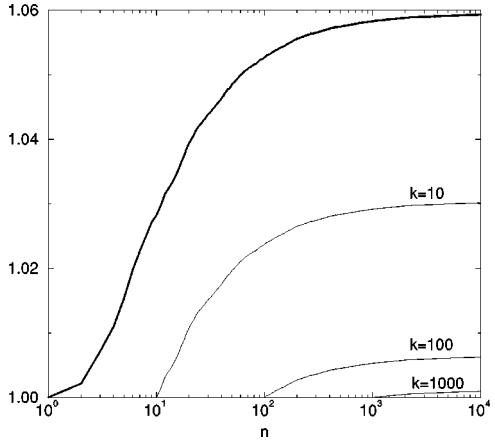

FIG. 8. The ratio of F_1 approximated by neglecting time correlations and the full F_1: $\Pi_{i=1}^{n}\langle(1+\lambda_i)^a\rangle/\langle\Pi_{i=1}^{n}(1+\lambda_i)^a\rangle$ (thick line). The quantities $\langle\Pi_{i=1}^{k}(1+\lambda_i)^a\rangle\Pi_{i=k+1}^{n}\langle(1+\lambda_i)^a\rangle$ are also plotted for $k=10$, 100, and 1000.

$$\langle F_1^{(n)}\rangle=\left\langle\prod_{i=1}^{n}(1+\lambda_i)^a\right\rangle \tag{48}$$

[see Eq. (13)]. Neglecting the correlations in time in the above product one may approximate

$$\left\langle\prod_{i=1}^{n}(1+\lambda_i)^a\right\rangle\approx\prod_{i=1}^{n}\langle(1+\lambda_i)^a\rangle. \tag{49}$$

Numerical evaluation of the two objects in Eq. (49) shows that they differ by a few percent (see Fig. 8). The numerics indicate the scaling laws

$$\left\langle\prod_{i=1}^{n}(1+\lambda_i)^a\right\rangle=c\lambda_0 n^{2/D}, \tag{50}$$

$$\prod_{i=1}^{n}\langle(1+\lambda_i)^a\rangle=c_1\lambda_0 n^{2/D}, \tag{51}$$

where $c_1/c\geqslant 1.06$.

To gain further insight we checked also the object

$$\left\langle\prod_{i=1}^{k}(1+\lambda_i)^a\right\rangle\prod_{i=k+1}^{n}\langle(1+\lambda_i)^a\rangle$$

for various values of k. The results are shown in Fig. 8. As it seems from this graph, time correlations between the initial and late stages of the growth are much more important than local correlations in the late stages.

We checked also two-point time correlations $\langle\lambda_n\lambda_{n-k}\rangle$ for some k's. The results are plotted in Fig. 9. As it turns out from this graph, $\langle\lambda_n\lambda_{n-k}\rangle\approx\langle\lambda_n\rangle\langle\lambda_{n-k}\rangle$ up to statistical fluctuations.

V. SUMMARY AND DISCUSSION

The language proposed by Hastings and Levitov appears to offer many appealing features. It generates DLA clusters in such a way that the conformal map $\Phi^{(n)}$ from the circle to the boundary of the cluster is known at every instant. In this paper we examined carefully the numerical procedure used to generate the conformal maps, and pointed out the advantages and the shortcoming of the algorithm.

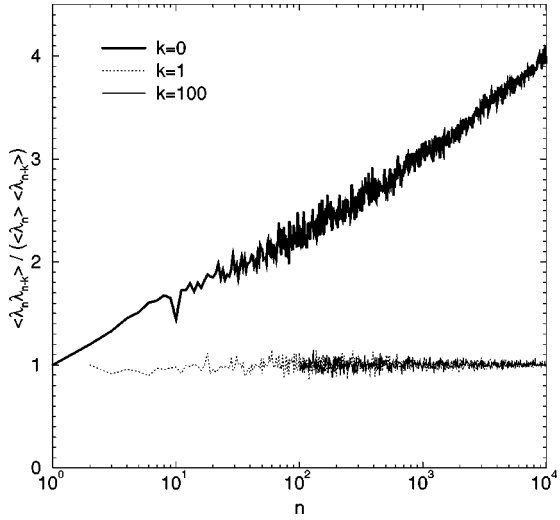

FIG. 9. Correlations of the field. In order to reduce statistical noise, the values plotted are averaged in bins $[n,1.01n]$.

The results of this paper pertain to the scaling behavior of the Laurent coefficients $|F_k|$ of the conformal map $\Phi^{(n)}$ and of the moments of λ_n which are related to moments of the field. We presented a theoretical discussion of the exponents characterizing moments of $|F_k|$ and λ_n. We pointed out the relations to the multifractal analysis of the harmonic measure, and derived scaling relations. Of particular interest is the scaling relation $D_3=D/2$ that was derived by Halsey and which appears here as a very natural consequence of the formalism.

One important result which is not adequately interpreted in this paper is the sharpness of the distribution of F_1. This coefficient is proportional to the radius of the cluster, and its sharpness is directly related to the existence of a universal fractal dimension independently of the details of the shape of the cluster. Understanding the sharpness appears to be connected to understanding the existence of universal fractal dimension, and we believe that it poses a very worthwhile and focused question for the immediate future.

ACKNOWLEDGMENTS

This work has been supported in part by the Israel Science Foundation founded by the Israel Academy of Sciences and Humanities. L.M.S. and E.S. are supported by U.S. DOE Grant No. DEFG-02-95ER-45546, and they would like to thank the Weizmann Institute of Science for hospitality.

APPENDIX A: CONSEQUENCES OF THE ONE-FOURTH THEOREM

In this appendix we prove that every univalent function of the type (11) is bounded in a circle of radius $4F_1$. This fact is based on two basic properties of univalent functions [13].

(1) There is one-to-one correspondence between univalent functions of the form $f(w)=a_1w+a_2w+\cdots$ (S class) and univalent functions of the form $g(w)=a_1w+a_{-1}/w+a_{-2}/w^2+\cdots$ (Σ class). This correspondence is given by

$$g(w)\leftrightarrow g(1/w)^{-1}. \tag{A1}$$

(2) The Koebe one-quarter theorem. *The image of the unit disk under every function of class S contains the disk* $z:|z|<4|a_1|$.

Consider a function $\Phi(w)$ of the form (11). This is a Σ-class function with linear coefficient F_1. Let us denote its conjugate [by Eq. (A1)] S-class function as $P(w)$. The linear coefficient of P is $1/F_1$. Consider now the smallest circle in the z plane which bounds the image of the unit circle under Φ, $\{z:|z|=R\}$. From Eq. (A1) it is clear that the circle $\{z:|z|=1/R\}$ is the largest circle which is contained in the image of the unit disk under P. Thus the Koebe one-quarter theorem ensures that $1/R\geqslant 1/(4F_1)$, which implies $R\leqslant 4F_1$.

APPENDIX B: ESTIMATE OF THE SCALING BEHAVIOR OF $\langle|F_{-k}^{(n)}|^2\rangle$

To estimate the large k and large n dependence of $F_{-k}^{(n)}$, the components are first written as integrals over the boundary of the cluster

$$F_{-k}^{(n)}=(1/2\pi)\int_0^{2\pi}\Phi^{(n)}(e^{i\theta})e^{ik\theta}d\theta$$

$$=\int_0^L z(s)e^{ik\theta(s)}|E(s)|ds, \tag{B1}$$

where

$$\theta(s)=\int_0^s|E(s')|ds'. \tag{B2}$$

For the purposes of Sec. IV we are interested in $|F_k^{(n)}|^2$:

$$|F_k^{(n)}|^2=\int_0^L\int_0^L z(s)z^*(s')e^{ik[\theta(s)-\theta(s')]}$$

$$\times|E(s)||E(s')|ds\,ds'. \tag{B3}$$

For a given value of n (or equivalently, of $R\sim n^{1/D}$), an examination of Eq. (B3) shows that for large k the fluctuations in the values of the integrands depend more crucially on the phase variations than on the field and radius variations. The phase varies appreciably when θ changes an amount

$$\Delta\theta\approx(\pi/2k) \tag{B4}$$

and therefore it is useful to split up the integral Eq. (B1) into a sum of essentially independent contributions coming from the electric field singularities with exponents α. This exponent is determined by the scaling law relating the measure (which is proportional to $\Delta\theta$) of a box to its size $(\Delta s)_\alpha$: $\Delta\theta\sim[(\Delta s)_\alpha/R]^\alpha$ [9]. The integral is split into contributions made of contour sections of different lengths $(\Delta s)_\alpha$ dependent on the singularity but each giving rise to the same change $\Delta\theta$. If one can estimate both the magnitude of the contribution of a specific multifractal electric field singularity α to the integral and the number of such contributions $\mathcal{N}_\alpha(k,n)$ [9], then one can write

$$\langle|F_{-k}^{(n)}|^2\rangle\sim\sum_j|I_{\alpha_j}(k,n)|^2$$

$$\sim\int d\alpha\,\mathcal{N}_\alpha(k,n)|I_\alpha(k,n)|^2, \tag{B5}$$

where

$$I_\alpha(k,n)\equiv\int_{(\Delta S)_\alpha}|E(s)|z(s)ds. \tag{B6}$$

To estimate $\mathcal{N}_\alpha(k,n)$ we recall that by definition

$$\Delta\theta=\int_s^{s+\Delta s}|E(s')|ds'\sim(\Delta s/R)^\alpha. \tag{B7}$$

From Eq. (B4)

$$(\Delta s)_\alpha\sim R(\pi/2k)^{1/\alpha}. \tag{B8}$$

Using Eq. (B8) and the fact that the fractal dimension of singularities of size α is $f(\alpha)$, we can now also estimate the number of singularities of size α which contribute to the integral as

$$\mathcal{N}_\alpha(k)\sim[R/(\Delta s)_\alpha]^{f(\alpha)}\sim(2k/\pi)^{f(\alpha)/\alpha}. \tag{B9}$$

To estimate $|I_\alpha(k,n)|^2$ we note that the major contribution to Eq. (B6) comes from the support of the harmonic measure where $|z(s)|\approx R$. Accordingly

$$|I_\alpha|^2\sim R^2\left[\int_{(\Delta s)_\alpha}|E(s)|ds\right]^2\sim R^2(\Delta\theta)^2\sim R^2(2\pi/k)^2, \tag{B10}$$

where we have made use of Eqs. (B2), (B4). Combining Eq. (B5) with the estimates (B9) and (B10) then yields

$$\langle|F_{-k}^{(n)}|^2\rangle\sim(R/4k)^2\int d\alpha(2k/\pi)^{f(\alpha)/\alpha}. \tag{B11}$$

We note that the approximation adopted in this appendix differs from the δ-function assumption (35) in asserting that for high values of k the variation of the phase dominates the decay of the integrand compared to the rapid decorrelation of the field. One would guess that for k of the order of unity the field decorrelates faster due to the rapid variation over the arc length. For high values of k the phase decorrelation is strongly amplified and we adopt the assumption used here.

[1] T. A. Witten and L. M. Sander, Phys. Rev. Lett. **47**, 1400 (1981).
[2] L. Niemeyer, L. Pietronero, and H. J. Wiesmann, Phys. Rev. Lett. **52**, 1033 (1984).
[3] L. Paterson, Phys. Rev. Lett. **52**, 1621 (1984).
[4] R. M. Brady and R. C. Ball, Nature (London) **309**, 225 (1984); D. Grier, E. Ben-Jacob, R. Clarke, and L. M. Sander, Phys. Rev. Lett. **56**, 1264 (1986).
[5] P. Meakin, in *Phase Transitions and Critical Phenomena*, edited by C. Domb and J. L. Lebowitz (Academic, New York, 1988), Vol. 12.
[6] A. Erzan, L. Pietronero, and A. Vespignani, Rev. Mod. Phys. **67**, 545 (1995).
[7] T. C. Halsey and M. Leibig, Phys. Rev. A **46**, 7793 (1992); T. C. Halsey, Phys. Rev. Lett. **72**, 1228 (1994).
[8] T. C. Halsey, P. Meakin, and I. Procaccia, Phys. Rev. Lett. **56**, 854 (1986).
[9] T. C. Halsey, M. H. Jensen, L. P. Kadanoff, I. Procaccia, and B. Shraiman, Phys. Rev. A **33**, 1141 (1986).
[10] M. B. Hastings and L. S. Levitov, Physica D **116**, 244 (1998).
[11] M. B. Hastings, Phys. Rev. E **55**, 135 (1997).
[12] R. C. Ball and R. M. Brady, J. Phys. A **18**, L809 (1985); S. Tolman and P. Meakin, Phys. Rev. A **40**, 428 (1988).
[13] P. L. Duren, *Univalent Functions* (Springer-Verlag, New York, 1983).
[14] H.G.E. Hentschel and I. Procaccia, Physica D **8**, 435 (1983).
[15] T. C. Halsey, Phys. Rev. Lett. **59**, 2067 (1987).